# Possible mechanism for limiting the number of modes in spin-wave instabilities in parallel pumping

S. P. Lim* and D. L. Huber
*Department of Physics, University of Wisconsin–Madison, Madison, Wisconsin 53706*
(Received 17 July 1989; revised manuscript received 25 September 1989)

Recent numerical studies of chaotic dynamics in magnetic systems have featured a small number of interacting modes. By applying the *S*-theory formalism of Zakharov *et al.*, we derive a set of dynamical equations that govern the behavior of the spin waves and their interactions for an easy-plane ferromagnet and an orthorhombic antiferromagnet under parallel-pumping conditions. All parameters in these equations are expressed in terms of the interaction constants of their respective microscopic Hamiltonian. Two distinguishing results follow from the analytical and numerical studies of these equations. First, the system tends to equilibrium states where only modes in a degenerate manifold are excited. The total population in this manifold is described by an analytic expression, but the individual occupation numbers are dependent on the initial conditions. Second, within this manifold, all spin-wave pair-correlation functions attain a common phase before the system reaches equilibrium. We refer to this phenomenon as "phase locking." In the presence of phase locking, we show that the approach to equilibrium for macroscopic number of modes is described by a pair of coupled first-order differential equations. These two results offer a possible mechanism for the reduction in the effective number of modes that could be used to describe such systems.

## I. INTRODUCTION

The phenomena of spin-wave instabilities have been intensely scrutinized since the early experiments of Damon[1] and Bloembergen and Wang,[2] where anomalies to the then-accepted notion of magnetic resonance were uncovered. The main features were satisfactorily explained by Suhl[3] for perpendicularly pumped ferromagnets. Spin waves were introduced to account for the experimental findings. Several years later, Zakharov *et al.*[4] presented a microscopic theory of the parametric excitation of spin waves, which subsequently became known as the *S* theory. Although the existence of low-frequency self-oscillations was observed in the early experiments, they were summarily dismissed. In the last few years, the existence of chaotic dynamics in nonlinear dissipative systems renewed interest in these self-oscillations. Since the class of experiments involving yttrium iron garnet (YIG) samples is among the cleanest and most readily modeled by well-known microscopic Hamiltonians, it is hoped that any new phenomena would shed more light on the understanding of such systems.

Armed with the *S* theory, Nakamura *et al.*[5] were the first to predict the existence of chaotic behavior in ferromagnets under a strong parallel oscillating microwave field. Gibson and Jeffries[6] were the first to report a period-doubling bifurcation in the oscillations of the absorbed-microwave power enroute to chaos. Their experiment was performed on YIG in the perpendicular-pumping configuration. Since then, various authors have investigated the nature of instabilities in spin waves both experimentally and numerically (see Refs. 7–12 and references therein). There is no doubt that such systems are rich in chaotic dynamics.

However, in all the preceding numerical case studies, the values of the parameters were chosen ad hoc and the numbers of modes were kept small. Although the few mode approximations were able to reproduce some of the primary features of the experiments, it is important to understand why this is the case. The works of Suhl and Zhang[11,13] and Gill and Zachary[14] are relevant here. In these papers arguments were made that an entire manifold of spin waves get excited. With these two points in mind, we chose to study a specific problem—that of an easy-plane ferromagnet with parallel static and oscillating fields that lie in the easy plane. Starting from a model microscopic Hamiltonian, we were able to express the parameters in the equations of the *S* theory in terms of the parameters of the Hamiltonian. With these specific parameters, the dynamical equations were studied numerically and analytically without restriction to a small number of modes. It was found that a thermal distribution of modes evolves into a single degenerate manifold. This manifold is situated at a value given by an explicit expression involving the parameters and the pumping strength of the microwave field. Within this manifold, the phases of each mode attain a common value before equilibrium is reached. We have referred to this phenomenon as "phase locking," and the related consequences have been reported in our earlier work.[15,16] We wish to concentrate here on showing the evolution to this single degenerate manifold and give an analytical argument for phase locking. We conclude with a discussion on how this could lead to a possible explanation for the fact that only a small number of modes need to be used to model chaos in magnetic systems.

 

An easy-plane ferromagnet with parallel static and microwave fields in the easy plane is modeled by the microscopic Hamiltonian

$$\mathcal{H}=-\sum_{i,j}' J\mathbf{S}_i\cdot\mathbf{S}_j+\sum_{i,j}' DS_i^xS_j^x-\mu gH\sum_j S_j^z +\mu gh\cos(\omega_p t)\sum_j S_j^z \ . \tag{1}$$

The primes signify summation over nearest neighbors only, and both the exchange integral $J$ and the anisotropy constant $D$ are positive. The third term is the Zeeman interaction and the last term represents the microwave field. The $S$ theory involves the ensemble averages of the following correlation functions of Bose operators, $c_k$ and $c_k^\dagger$, that diagonalize the zeroth-order Hamiltonian

$$\langle c_k^\dagger(t)c_k(t)\rangle=n_k(t) \ ,$$

$$\langle c_k(t)c_{-k}(t)\rangle=\sigma_k(t)e^{i\omega_p t} \ .$$

After a time of order $1/\gamma_k$, where $\gamma_k$ is the decay rate for the $k$th spin wave, the system evolves to a regime where the phases of the spin-wave pair are fully correlated.[4,17] In this case we have $n_k=n_{-k}$ and $|\sigma_k|=n_k$, which we can write in terms of $n_k$ and a phase $\psi_k$:

$$\sigma_k=n_k e^{i\psi_k} \ .$$

In terms of $n_k$ and $\psi_k$, the equations of motion assume the form[15]

$$\frac{1}{2}\frac{dn_k}{dt}=n_k[-\gamma+V\sin\psi_k+T\sum_{k'} n_{k'}\sin(\psi_k-\psi_{k'})] \ , \tag{2}$$

$$\frac{1}{2}\frac{d\psi_k}{dt}=\omega_k-\frac{\omega_p}{2}+2T\sum_{k'}n_{k'}+V\cos\psi_k +T\sum_{k'}n_{k'}\cos(\psi_k-\psi_{k'}) \ , \tag{3}$$

with

$$V=\frac{DSz}{4}\frac{\mu gH}{[\mu gH(\mu gH+2DSz)]^{1/2}} \ ,$$

$$T=-\frac{Dz}{4N}\left[\frac{2\mu gH+DSz}{\mu gH+2DSz}\right] \ ,$$

$$\omega_k=\{[2JSz(1-\lambda_k)+\mu gH +2DSz\lambda_k][2JSz(1-\lambda_k)+\mu gH]\}^{1/2} \ ,$$

$$\lambda_k=\frac{1}{z}\sum_\delta e^{i\mathbf{k}\cdot\delta} \ ,$$

where $z$ is the number of nearest neighbors and $\delta$ connects the nearest neighbors. $N$ is the total number of spins in the system. The preceding equations of motion are somewhat simplified—the decay rates are the same for all modes and the values of $V$ and $T$ are all taken as that of the $\mathbf{k}=0$ mode (long-wavelength approximation). With these assumptions, we are now ready to address the problem.

## II. ANALYSIS

We first study the system of equations (2) and (3) without the nonlinear terms

$$\frac{1}{2}\frac{dn_k}{dt}=n_k(-\gamma+V\sin\psi_k) \ , \tag{4}$$

$$\frac{1}{2}\frac{d\psi_k}{dt}=\Delta\omega_k+V\cos\psi_k \ , \tag{5}$$

with $\Delta\omega_k=\omega_k-\omega_p/2$. Equation (5) has two solutions[18] that depend on the values of $V$ and $\Delta\omega_k$.

(1) For $\Delta\omega_k^2>V^2$, we have the solution

$$\frac{2}{(\Delta\omega_k^2-V^2)^{1/2}}\tan^{-1}\frac{(\Delta\omega_k^2-V^2)\tan(\psi_k/2)}{\Delta\omega_k+V}=2(t+c) \ ,$$

where $c$ is the constant of integration. From Eq. (4) we have

$$\frac{1}{2}\frac{dn_k}{dt}=\left\{-\gamma+\frac{2V(\Delta\omega_k^2-V^2)\tan[(\Delta\omega_k^2-V^2)^{1/2}(t+c)]}{\Delta\omega_k-V+(\Delta\omega_k+V)\tan^2[(\Delta\omega_k^2-V^2)^{1/2}(t+c)]}\right\}n_k \ .$$

Since the tangent is a periodic function, when averaged over time the time-dependent part is zero; so

$$\left\langle\frac{1}{2}\frac{dn_k}{dt}\right\rangle_t=-\gamma\langle n_k\rangle_t \ , \tag{6}$$

implying that $n_k(t)$ tends to zero for $\gamma t\gg 1$.

(2) For $\Delta\omega_k^2<V^2$, the solution is

$$\frac{1}{(V^2-\Delta\omega_k^2)^{1/2}}\ln\frac{(V^2-\Delta\omega_k^2)^{1/2}\tan(\psi_k/2)+V+\Delta\omega_k}{(V^2-\Delta\omega_k^2)^{1/2}\tan(\psi_k/2)-V-\Delta\omega_k}=2(t+c) \ ,$$

where once again $c$ is the constant of integration. Then Eq. (4) results in

$$\frac{1}{2}\frac{dn_t}{dt}=\left\{-\gamma+\frac{2V(V^2-\Delta\omega_k^2)^{1/2}\tanh[(V^2-\Delta\omega_k^2)^{1/2}(t+c)]}{V+\Delta\omega_k+(V-\Delta\omega_k)\tanh^2[(V^2-\Delta\omega_k^2)^{1/2}(t+c)]}\right\}n_k \ .$$

As $t\rightarrow\infty$,

$$\tanh[(V^2-\Delta\omega_k^2)^{1/2}(t+c)]\rightarrow 1$$

so that

$$\frac{1}{2}\frac{dn_k}{dt}\rightarrow[-\gamma+(V^2-\Delta\omega_k^2)^{1/2}]n_k \ .$$

For growth, we must have $-\gamma+(V^2-\Delta\omega_k^2)^{1/2}>0$ or

$$-(V^2-\gamma^2)^{1/2}<\Delta\omega_k<(V^2-\gamma^2)^{1/2} \ . \tag{7}$$

Equation (7) defines the range of $\Delta\omega_k$ for which growth is possible. The maximum value for $dn_k/2dt$ occurs when $\Delta\omega_k=0$. This analysis shows that there is an instability threshold when $V>\gamma$ and that the modes around $\Delta\omega_k=0$ are the ones that get excited (see Fig. 1).

If we now include the nonlinear terms, it can be readily shown that the equations of motion can be put in the form

$$\frac{1}{2}\frac{dn_k}{dt}=[-\gamma+A\sin(\psi_k-\theta)]n_k \ , \tag{8}$$

$$\frac{1}{2}\frac{d\psi_k}{dt}=\Delta\tilde{\omega}_k+A\cos(\psi_k-\theta) \ , \tag{9}$$

where

$$A^2=(V+T\sum_k n_k\cos\psi_k)^2+(T\sum_k n_k\sin\psi_k)^2 \ ,$$

$$\Delta\tilde{\omega}_k=\Delta\omega_k+2T\sum_{k'}n_k \ ,$$

$$\theta=\tan^{-1}\frac{T\sum_{k'}n_{k'}\sin\psi_{k'}}{V+T\sum_{k'}n_{k'}\cos\psi_{k'}} \ .$$

We see that these equations have the same form as the linear equations provided the time interval is small enough that $d\theta/dt\simeq 0$ and $d\Delta\tilde{\omega}_k/dt\simeq 0$. In this regime, the modes that grow, by analogy, are those confined to the interval

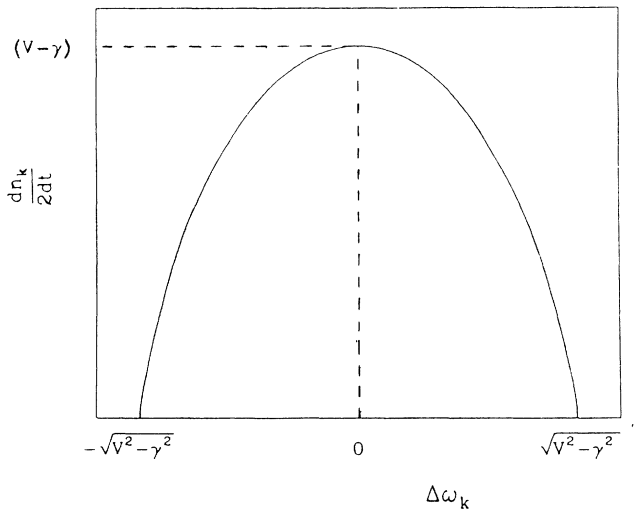


FIG. 1. Plot of $dn_k/2dt$ vs $\Delta\omega_k$ in linear approximation. This shows range where $dn_k/2dt$ is positive.

$$-(A^2-\gamma^2)^{1/2}<\Delta\tilde{\omega}_k<(A^2-\gamma^2)^{1/2} \ . \tag{10}$$

We now conjecture that there is a single mode, denoted by the wave vector $\mathbf{k}_0$, which is a stable fixed point of this system of equations, and that all other modes suffer decay in time. If this is the case, since (10) denotes a band of growth, this band must be of zero width. In other words, we have

$$A^2=\gamma^2 \text{ and } \Delta\tilde{\omega}_{k_0}=0 \ . \tag{11}$$

For this mode to be a fixed point, $dn_{k_0}/dt=0$ and $d\psi_{k_0}/dt=0$. These two conditions together with Eqs. (9) and (11) can be solved to give[4]

$$n_{k_0}=-\frac{1}{T}(V^2-\gamma^2)^{1/2} \ ,$$

$$\psi_{k_0}=\sin^{-1}\frac{\gamma}{V} \ ,$$

$$\Delta\omega_{k_0}=-2Tn_{k_0} \ ,$$

which are seen to be independent of the initial conditions. Note that since $T<0$, the value of $n_{k_0}$ is positive (for physically realizable states). In order to prove our conjecture, we will show that this fixed point is stable. By performing a linear stability analysis, we show that any small deviation from the fixed point decays away exponentially; this proves our conjecture. We rewrite Eqs. (2) and (3),

$$\frac{1}{2}\frac{dn_k}{dt}=[-\gamma+(V+T\sum_{k'}n_{k'}\cos\psi_{k'})\sin\psi_k-(T\sum_{k'}\sin\psi_{k'})\cos\psi_k]n_k \ ,$$

$$\frac{1}{2}\frac{d\psi_k}{dt}=\Delta\omega_k+2T\sum_{k'}n_{k'}+(V+T\sum_{k'}n_{k'}\cos\psi_{k'})\cos\psi_k+(T\sum_{k'}n_{k'}\sin\psi_{k'})\sin\psi_{k'} \ .$$

Now define

$$X=\sum_k n_k\sin\psi_k \ ,$$

$$Y=\sum_k n_k\cos\psi_k \ ,$$

$$N_T=\sum_k n_k \ .$$

Then one can readily show that

$$\tfrac{1}{2}\frac{d}{dt}X=-\gamma X+(V+3TY)N_T+\sum_k\Delta\omega_k n_k\cos\psi_k \ , \tag{12}$$

$$\tfrac{1}{2}\frac{d}{dt}Y=-\gamma Y+3TXN_T-\sum_k\Delta\omega_k n_k\sin\psi_k \ , \tag{13}$$

$$\tfrac{1}{2}\frac{d}{dt}N_T=-\gamma N_T+VX \ . \tag{14}$$

Now consider the case where only a narrow band of modes around the mode $\mathbf{k}_0$ are macroscopically occupied. Then we can approximate $\Delta\omega_k\approx\Delta\omega_{k_0}=-2Tn_{k_0}$. For small deviations about the fixed point with

$n_{k_0}=-V\cos\psi_{k_0}/T$ and $\psi_{k_0}=\sin^{-1}(\gamma/V)$, we define the following:

$$N_T=N_{k_0}+\Delta N_T ,$$
$$Y=n_{k_0}\cos\psi_{k_0}+\Delta_c ,$$
$$X=n_{k_0}\sin\psi_{k_0}+\Delta_s ,$$

where the quantities $\Delta N_T$, $\Delta_c$, and $\Delta_s$ are small deviations. To the lowest order in these quantities, the equations of motion are

$$\tfrac{1}{2}d\Delta N_T/dt=-\gamma\Delta N_T+V\Delta_s ,$$
$$\tfrac{1}{2}d\Delta_s/dt=3Tn_{k_0}(\cos\psi_{k_0})\Delta N_T+Tn_{k_0}\Delta_c-\gamma\Delta_s ,$$
$$\tfrac{1}{2}d\Delta_c/dt=3Tn_{k_0}(\sin\psi_{k_0})\Delta N_T-Tn_{k_0}\Delta_s-\gamma\Delta_c ,$$

The solution to the preceding equations is of the form

$$\Delta_s(t)=s_1e^{-2(\gamma-a-b)t}+[s_2e^{i\sqrt{3}/2(a-b)t}+s_3e^{-i\sqrt{3}/2(a-b)t}]e^{-(2\gamma+a+b)t} ,$$
$$\Delta_c(t)=c_1e^{-2(\gamma-a-b)t}+[c_2e^{i\sqrt{3}/2(a-b)t}+c_3e^{-i\sqrt{3}/2(a-b)t}]e^{-(2\gamma+a+b)t} ,$$
$$\Delta N_T(t)=n_1e^{-2(\gamma-a-b)t}+[n_2e^{i\sqrt{3}/2(a-b)t}+n_3e^{-i\sqrt{3}/2(a-b)t}]e^{-(2\gamma+a+b)t} ,$$

where $n_i$, $c_i$, and $s_i$, $i=1,2,3$ are constants and

$$a=[(V^2-\gamma^2)\{-3\gamma/2+[\tfrac{9}{4}\gamma^2+\tfrac{64}{27}(V^2-\gamma^2)]^{1/2}\}]^{1/3} ,$$
$$b=[(V^2-\gamma^2)\{-3\gamma/2-[\tfrac{9}{4}\gamma^2+\tfrac{64}{27}(V^2-\gamma^2)]^{1/2}\}]^{1/3} .$$

It can readily be shown that $\gamma-a-b>0$ and $2\gamma+a+b>0$ for all values of $V>\gamma$. Hence all deviations decay in time. As already shown, for $\Delta\tilde{\omega}_k^2>A^2$, $\frac{1}{2}dn_k/dt<0$ so these modes decay. For $\Delta\tilde{\omega}_k^2<A^2$, when situated around the fixed point $\mathbf{k}_0$, an explicit solution for this band of modes is

$$n_k(t)=n_k(0)\exp\{[(\Delta_k^2/Y)+2T\sin\psi_{k_0}\Delta_c-2T\cos\psi_{k_0}\Delta_s-4T\Delta_k\Delta N_T]t\} ,$$

with $\Delta_k\equiv\omega_k-\omega_{k_0}$. As $\Delta_c$, $\Delta_s$, and $\Delta N_T$ all decay exponentially with time, the above shows that all modes away from $\mathbf{k}_0$ (i.e., $\Delta_k\neq0$) decay in time, whereas $\mathbf{k}_0$ itself is stable. This proves our conjecture.

The question now arises—how does the system evolve to the state where only the stable mode is macroscopically occupied? The analysis leading to Eq. (10) shows that the band that gets excited is centered around $\Delta\tilde{\omega}_k$ $(=\omega_k-\omega_p/2+2T\sum_{k'}n_{k'})$ so at the early states of pumping, only those modes near $\omega_p/2$ get excited. We now show that given any macroscopically excited mode that is not the stable mode $\mathbf{k}_0$, the system will shift towards $\mathbf{k}_0$.

Assume there is one dominant mode $\mathbf{k}\neq\mathbf{k}_0$, for simplicity. Then one can readily see that for this case,

$$\psi_k\simeq\psi_{k_0} ,$$
$$n_k\simeq\frac{\Delta\omega_k+V\cos\psi_{k_0}}{3T} .$$

For any mode $\mathbf{k}'\neq\mathbf{k}$, the preceding conditions give

$$\frac{1}{2}\frac{dn_{k'}}{dt}=\left\{-\gamma+\left[\gamma^2+\left[\frac{\Delta_k}{3}\right]\right]^{1/2}\sin(\psi_{k'}-\psi_{k_0}-\beta)\right\}n_{k'} , \tag{15}$$

$$\frac{1}{2}\frac{d\psi_{k'}}{dt}=\Delta_{k'}-\frac{\Delta_k}{3}-\left[\gamma^2+\left[\frac{\Delta_k}{3}\right]^{1/2}\cos(\psi_{k'}-\psi_{k_0}-\beta)\right] , \tag{16}$$

where $\beta=\tan^{-1}(3\gamma/\Delta_k)$. Note that for $\mathbf{k}=\mathbf{k}_0$, the system is already at the stable position ($\Delta_k=0$) so that Eq. (15) gives $\frac{1}{2}(dn_{k'}/dt)<0$, as should be the case. Once again we can solve these equations.

(1) For $(\Delta_{k'}-\Delta_k/3)^2>\gamma^2+(\Delta_k/3)^2$, the arguments leading to Eq. (6) once again result in $\frac{1}{2}\langle n_{k'}\rangle_t=-\gamma\langle n_k\rangle_t$ so that modes in this range suffer exponential decay.

(2) For

$$\left[\Delta_{k'}-\frac{\Delta_k}{3}\right]^2<\gamma^2+\left[\frac{\Delta_k}{3}\right]^2 ,$$

we get

$$\frac{1}{2}\frac{dn_{k'}}{dt}=\left\{-\gamma+\frac{2E(E^2-\nu_{k'}^2)^{1/2}\tanh[(E^2-\nu_{k'}^2)^{1/2}(t+c)]}{E-\nu_{k'}+(E+\nu_{k'})\tanh^2[(E^2-\nu_{k'}^2)^{1/2}(t+c)]}\right\}n_{k'} ,$$

with $E=[\gamma^2+(\Delta_k/3)^2]^{1/2}$, $v_{k'}=\Delta_{k'}-2\Delta_k/3$ and $c$ is a constant of integration. For large values of $t$,

$$\tfrac{1}{2}n_{k'}\rightarrow\{-\gamma+[\gamma^2+(\Delta_k/3)^2-(\Delta_{k'}-2\Delta_k/3)^2]^{1/2}\}n_{k'}$$

so that $\frac{1}{2}dn_{k'}/dt$ is symmetric about its maximum value of

$$\{[\gamma^2+(\Delta_k/3)^2]^{1/2}-\gamma\}n_{k'}$$

centered at $\Delta_{k'}=2\Delta_k/3$. For modes to grow, we require

$$[\gamma^2+(\Delta_k/3)^2-(\Delta_{k'}-2\Delta_k/3)^2]^{1/2}>\gamma\ .$$

This translates to

$$\tfrac{2}{3}\Delta_k-\frac{|\Delta_k|}{3}<\Delta_{k'}<\tfrac{2}{3}\Delta_k+\frac{|\Delta_k|}{3}\ .$$

We now consider two cases.

(a) $\Delta_k>0$ (the present peak is above the stable fixed mode $\mathbf{k}_0$). Then $\frac{1}{2}dn_{k'}/dt>0$ when

$$\tfrac{1}{3}|\Delta_k|<\Delta_{k'}<|\Delta_k| \quad \text{or} \quad \omega_{k_0}+\tfrac{1}{3}|\Delta_k|<\omega_{k'}<\omega_k\ .$$

This is illustrated in Fig. 2.

(b) $\Delta_k<0$ (the present peak is below the stable fixed mode $\mathbf{k}_0$). Then $\frac{1}{2}dn_{k'}/dt>0$ when

$$-|\Delta_k|<\Delta_{k'}<-\tfrac{1}{3}|\Delta_k| \quad \text{or} \quad \omega_k<\omega_{k'}<\omega_{k_0}-\tfrac{1}{3}|\Delta_k|\ .$$

This is illustrated in Fig. 3.

Thus we see that if the dominant mode is above the stable fixed point, the band with a positive growth rate is below the dominant mode. The converse is true if the dominant mode is below the stable mode. All other modes decay away. In both cases, the width of the band of growth is $\frac{2}{3}|\Delta_k|$ so that the closer the dominant mode is to the stable mode, the narrower is this band. Also the maximum growth rate within the band,

$$2\left\{\left[\gamma^2+\left[\frac{\Delta_k}{3}\right]^2\right]^{1/2}-\gamma\right\}n_{k'}\ .$$

is smaller the closer the dominant mode is to the stable mode. We offer numerical evidence for this behavior. Solving the set of coupled equations (2) and (3) with a uniform distribution of modes and arbitrary initial conditions, we see that the system evolves towards the stable peak $\mathbf{k}_0$. Figures 4 and 5 illustrate this for the two different cases: one when the dominant mode is above $\mathbf{k}_0$ and the other when it is below $\mathbf{k}_0$. Also indicated are the values of $\omega_{k_0}$ and $n_{k_0}$.

What happens if there are other modes that are degenerate or very close in energy to $\mathbf{k}_0$? To answer this question we go back to Eqs. (12), (13), and (14). These can be manipulated to give

$$\frac{1}{4}\frac{d}{dt}(X^2+Y^2-N_T^2)=-\gamma(X^2+Y^2-N_T^2)+\sum_{k,k'}\Delta\omega_k n_k n_{k'}\sin(\psi_k-\psi_{k'})\ . \quad (17)$$

It has been established that $\mathbf{k}_0$ is a stable mode. For modes very close to $\mathbf{k}_0$, $\Delta\omega_k\simeq\Delta\omega_{k_0}=$constant. In this case, the second term is identically zero. Hence

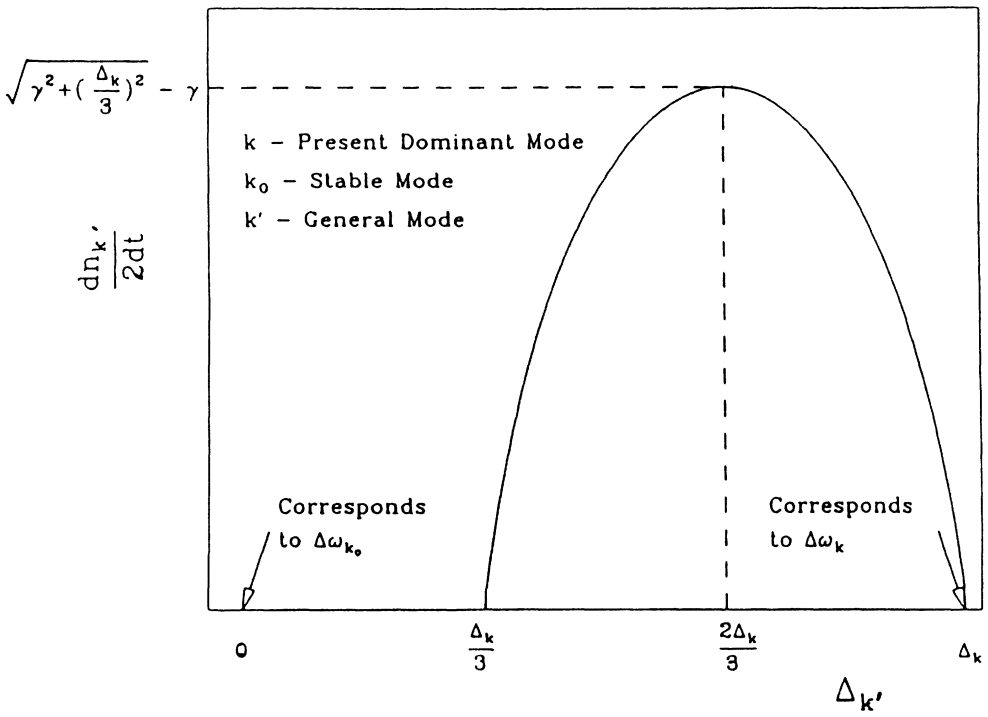


FIG. 2. Plot of $dn_{k'}/2dt$ vs $\Delta_{k'}$ for $\Delta_k>0$ when nonlinear terms are included. This shows band of positive growth for $dn_{k'}/2dt$.

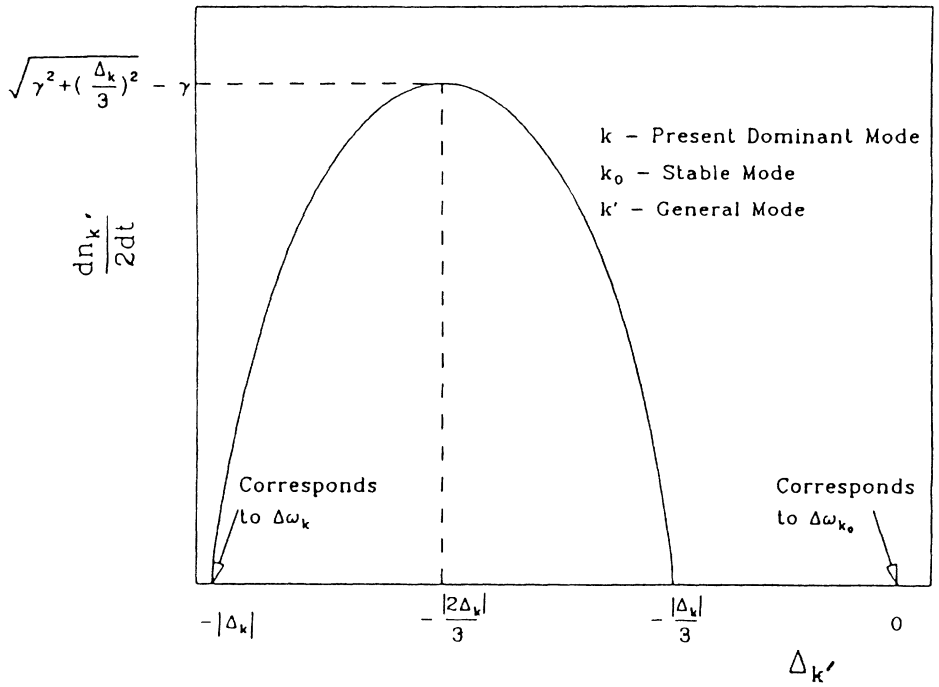


FIG. 3. Plot of $dn_{k'}/2dt$ vs $\Delta_k'$ for $\Delta_k < 0$ when nonlinear terms are included. This shows band of positive growth for $dn_{k'}/2dt$.

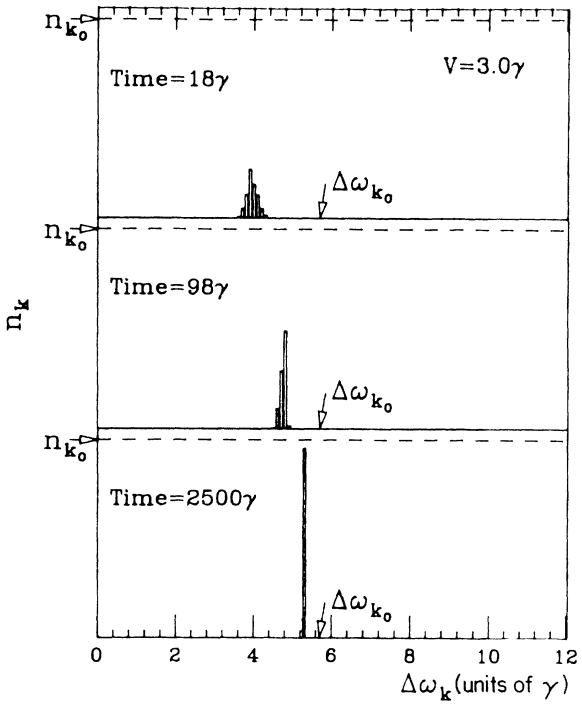


FIG. 4. Profile of magnon population at various times only nondegenerate modes are shown. One hundred modes are included. Initial conditions were chosen so that steady state is approached from below. $V=3\gamma$, $T=-\gamma$. Also shown are $N_0=-(V^2-\gamma^2)^{1/2}/T$ and $\omega_{k0}$, the analytical equilibrium values.

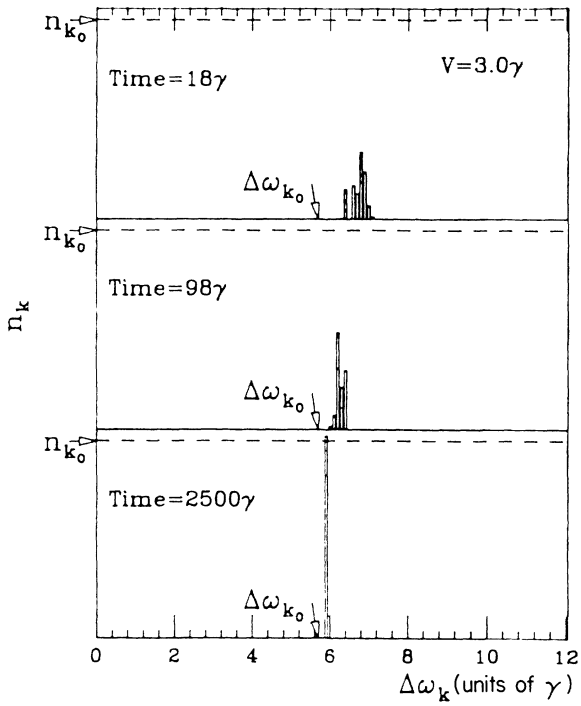


FIG. 5. Profile of magnon population at various times only nondegenerate modes are shown. One hundred modes are included. Initial conditions were chosen so that steady state is approached from above. $V=3\gamma$, $T=-\gamma$. Also shown are $N_0=-(V^2-\gamma^2)^{1/2}/T$ and $\omega_{k0}$, the analytical equilibrium values.

$$\frac{1}{4}\frac{d}{dt}(X^2+Y^2-N_T^2)\rightarrow-\gamma(X^2+Y^2-N_T^2)$$

implying that

$$(\sum_k n_k\sin\psi_k)^2+(\sum_k n_k\cos\psi_k)^2\underset{t\rightarrow\infty}{\rightarrow}(\sum_k n_k)^2 ,$$

or

$$\sum_{k,k'} n_k n_{k'}[\cos(\psi_k-\psi_{k'})-1]\underset{t\rightarrow\infty}{\rightarrow}0 .$$

For $\mathbf{k}=\mathbf{k}'$, this is identically satisfied. For $\mathbf{k}\neq\mathbf{k}'$, the preceding implies that all modes that are close to $\mathbf{k}_0$ must either be unoccupied or else they have equal phases. That is, $\psi_k=\psi_{k'}\mathrm{mod}2\pi$, for all macroscopically occupied pairs $\mathbf{k}$ and $\mathbf{k}'$ when they are degenerate (or nearly so). We refer to this as "phase locking." Equation (17) shows that phase locking occurs on a time scale of $\frac{1}{4}\gamma$. The threshold for instability is at $V>\gamma$. In the limit as $V\rightarrow\infty$, it can be readily shown that $\sum_k n_k(t)$ approaches its equilibrium value at a rate of $1/\gamma$. For small values of $V$, the rate is much slower. Hence it is safe to conclude that phase locking is not a steady-state result but should happen before equilibrium is established. This has been confirmed by our previous work (see Refs. 15 and 16). If we use this fact in our analysis that leads to the stable mode $\mathbf{k}_0$ already given, what we get instead is a whole manifold $m$ of stable almost-degenerate modes. We then have

$$\psi_{k\in m}=\psi_{k_0}=\sin^{-1}\frac{\gamma}{V} , \tag{18}$$

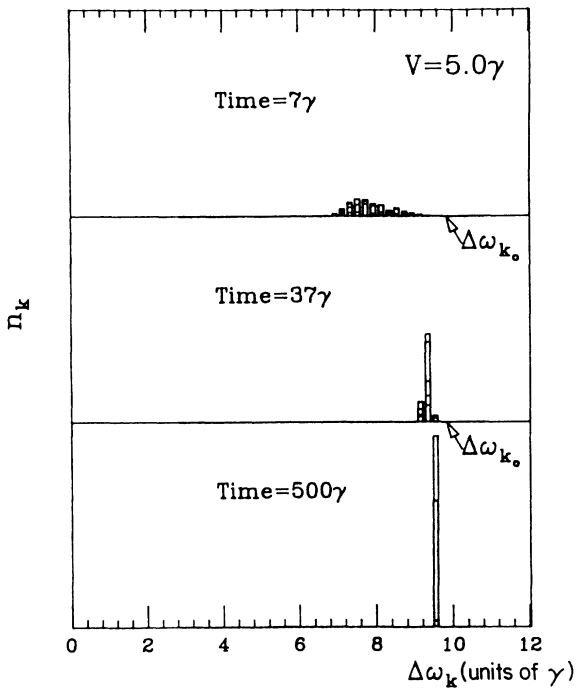


FIG. 6. Profile of magnon population for forty sets of degenerate modes, each set having five modes. $V=5\gamma$, $T=-\gamma$. This result is typical of a single run with arbitrary initial conditions.

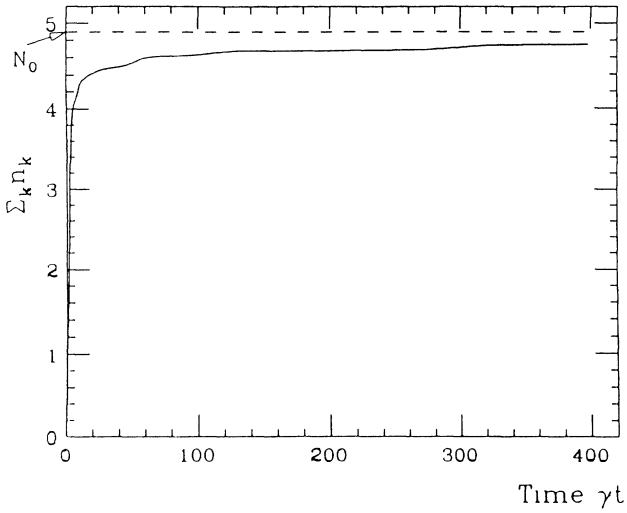


FIG. 7. Total population of magnon modes (at the same conditions as Fig. 6) vs time. Also shown are $N_0=-(V^2-\gamma^2)^{1/2}/T$ and $\omega_{k0}$, the analytical equilibrium values.

$$\sum_{k\in m} n_k=-\frac{1}{T}(V^2-\gamma^2)^{1/2} , \tag{19}$$

$$\Delta\omega_{k\in m}=-2T\sum_{k\in m} n_k=2(V^2-\gamma^2)^{1/2} . \tag{20}$$

We conclude here that in the system being pumped a set of modes are selectively excited, consistent with Eqs. (19) and (20). Numerically, the relative values of the occupation numbers of the different modes within this manifold depend on the initial conditions but the sum of all the occupation numbers obeys

$$\sum_{k\in m} n_k=-\frac{1}{T}(V^2-\gamma^2)^{1/2} .$$

(See Figs. 6 and 7).

## III. GENERALIZATION

Given that our system evolves towards the stable manifold determined by Eq. (20), what happens if this condition cannot be satisfied because of a gap in the energy spectrum? What we expect and find to be the case numerically is the same evolution towards the stable manifold except that the system piles up at the edge of the gap. See Figs. 8 and 9. When this happens, the degenerate manifold at the edge simply builds up to a certain level and remains a stable point of the system. This is equivalent to the case of a constant $\Delta\omega_k$ when $\Delta\omega_k$ is the value at the edge of the gap. This is exactly the case we have studied earlier (see Refs. 15 and 16). All the results there carry over even to the case when $\Delta\tilde{\omega}_k=0$ is satisfied, which is a special case of the constant-$\Delta\omega_k$ case. We quote the main results. At the fixed point [be it given by Eq. (20) or edge of gap],

$$\psi^0_{k\in m}=\sin^{-1}\frac{\gamma}{V} ,$$

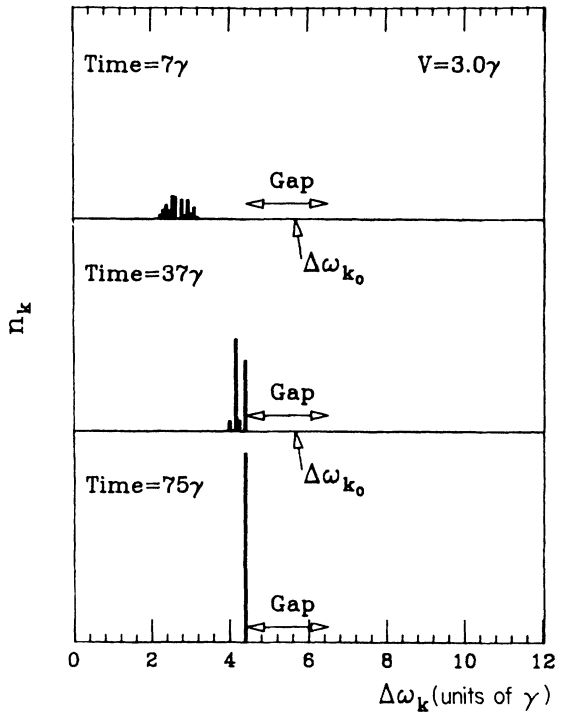


FIG. 8. Profile of magnon population at various times with gap. Final steady state is below the peak mode which is in the gap. There are fifty modes each above and below the gap. $V=3\gamma$, $T=-\gamma$.

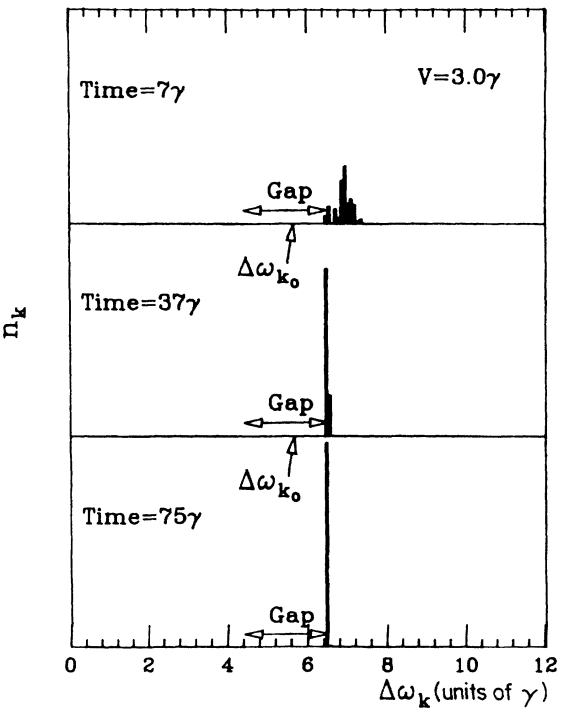


FIG. 9. Profile of magnon population at various times with gap. Final steady state is above the peak mode which is in the gap. There are fifty modes each above and below the gap. $V=3\gamma$, $T=-\gamma$.

$$\sum_{k\in m} n_k^0 = \frac{-\Delta\omega - V\cos\psi^0}{3T} .$$

This fixed point is stable against small perturbations. For small values above threshold, evolution towards the stable fixed point is exponential, and for larger values, the system exhibits damped oscillatory behavior. The crossover value of pumping-field strength $V$ agrees fairly well with that obtained from a linear stability analysis. The behavior does not depend qualitatively on the number of modes considered. We have investigated this up to 150 modes. Phase locking is observed numerically in all cases, with no exception. With phase locking we can actually reduce the large number of equations considered to two:

$$\frac{1}{2}\frac{dN_T}{dt} = N_T(-\gamma + V\sin\psi) ,$$

$$\frac{1}{2}\frac{d\psi}{dt} = \Delta\omega + 3N_T T + V\cos\psi .$$

Since the parameters in the system are fixed by the parameters of the microscopic Hamiltonian, we have no freedom to vary them. For this set of equations, no chaotic behavior was found. We have also studied the orthorhombic antiferromagnet, which under certain conditions, yields an identical set of equations (see the Appendix).

## IV. DISCUSSION

From our analysis, we learn that under parallel-pumping conditions a ferromagnet with easy-plane anisotropy and the orthorhombic antiferromagnet evolve to a stable state where a single manifold of degenerate modes are excited. Within this manifold the individual occupation numbers cannot be determined since they depend on the initial conditions.[19] However the sum of all these occupation numbers, which is directly related to the measured magnetization, is a well-defined number. The important phenomenon phase locking enables us to treat this single manifold as a single mode. This reduction, which is accomplished first through the evolution of the system to a degenerate manifold and second through phase locking, is of particular interest. The theoretical and numerical studies of the various above-mentioned authors assumed only a very small number of modes in their work. As far as our results indicate, there is no difference in the total occupation number whether we have two modes or more than a hundred. Since the total occupation number is the connection between theory and experiment, like those of the previous authors, our results could also be modeled by a two-mode system.

With ad hoc choices for the parameters, many experimental features were simulated numerically with low-dimensional systems. This has prompted the belief that such systems can be described by only a few variables. The effective reduction in the number of modes through phase locking may offer just such an explanation. If the macroscopic number of modes that are excited are concentrated around two degenerate manifolds, then phase locking would "reduce" this down to an effective-two-

mode system, where one represents each manifold. Although derived from a microscopic Hamiltonian, our $S$ and $T$ parameters in the $S$ theory are calculated only in the long-wavelength limit. Should the two degenerate manifolds be far apart so that the $\mathbf{k}$ dependence of $S$ and $T$ becomes significant, we can have different $S$ and $T$ values that connect the different manifolds so that chaotic dynamics may result. However, in the long-wavelength regime we find only one degenerate manifold in our system. It may be this lack of multiple manifolds, and hence lack of possibly different parameters connecting them, that leads to our failure to observe chaos.

Recently, Suhl and Zhang analyzed a number of high-power effects in ferromagnetic resonance using an approach that is largely complementary to the analysis presented here.[20,21] In their characterization of parallel pumping, they neglect detuning and assume a single dominant mode. There is coupling between the dominant mode and each of the inferior modes, but not among the inferior modes themselves. Such a model is qualitatively similar to the limiting behavior outlined in Sec. II. In a sense, the results in this paper show how the system evolves in time to a point where the Suhl-Zhang approximation is appropriate.

The analysis of Suhl and Zhang was based in part on center-manifold theory, which provides a systematic method for approximating the effect of the decaying modes on the evolution of the unstable modes.[22] Such an approach can presumably be applied to the model discussed in this paper. However, the analysis is likely to be even more complicated than what was outlined in Ref. 21, and thus far more complicated than our own approach, since a central feature of our model is the continuous distribution of spin-wave frequencies. This leads to a situation where the modes with growing amplitudes change with time [cf. Eq. (15)]. Furthermore, even in the case of a degenerate spin-wave manifold, the application of center-manifold theory is not without problems.[21]

The Suhl-Zhang analysis is also complementary to the treatment of parallel pumping given in Refs. 15 and 16. There it was assumed that all modes had the same detuning and the same interactions, in contrast to the dominant-mode scenario. According to the $S$ theory, with common detuning and interactions, the phases become locked, and the total magnon population approaches an asymptotic value determined by $V$, $\gamma$, $\Delta\omega$, and $T$, independent of initial conditions.


## ACKNOWLEDGMENTS

This research was supported in part by the National Science Foundation.


## APPENDIX: ORTHORHOMBIC ANTIFERROMAGNET

In this Appendix we will derive the equations of motion for the case of an orthorhombic antiferromagnet that is characterized by different effective fields for displacements in the $x$ and $y$ directions. This is represented by the microscopic Hamiltonian

$$\mathcal{H}=J\sum_{j,\delta}\mathbf{S}_j\cdot\mathbf{S}_{j+\delta}+\mu gH\sum_j S_j^z+K_1\sum_j (S_j^x)^2+K_2\sum_j (S_j^y)^2 , \tag{A1}$$

where $j$ is summed over two sublattices, and $\delta$ connects nearest neighbors that are from different sublattices. $H$ is the usual Zeeman field and $J$ is the positive exchange energy. $K_1$ and $K_2$ are positive and represent the anisotropy energies in the $x$ and $y$ directions, respectively. The positive exchange energy means that spins next to one another tend to line up antiparallel so, unlike the ferromagnetic case, we have two intermeshed sublattices of spins. Within each sublattice, the spins are parallel but one sublattice lines up antiparallel to the other. The best way to describe this system is to denote each sublattice differently. Let the Zeeman field denote the positive direction so that one sublattice points along it and the other antiparallel to it. Then the elementary excitations in the two sublattices consist of deviations from the positive $z$ axis in one case and the negative $z$ axis in the other. Hence the Holstein-Primakoff transformations in this case are

$$S_j^+=(2S-a_j^\dagger a_j)^{1/2}a_j ,$$
$$S_j^+=b_j^\dagger(2S-b_j^\dagger b_j)^{1/2} ,$$

where $a_j$ is the atomic-annihilation operator for the sublattice that points along the $z$ axis and $b_j$ that for the sublattice that points antiparallel to the $z$ axis. We have assumed that both sublattices have equal spin magnitude $S$. On applying these transformations, keeping second-order terms and expressing the results in terms of spin-wave coordinates, we get

$$\mathcal{H}=\mathcal{H}_0+\mathcal{H}_1+\mathcal{H}_2 ,$$

where $\mathcal{H}_0$ is a constant and

$$\mathcal{H}_1=\sum_k 2JSz\lambda_k(a_k b_k+a_k^\dagger b_k^\dagger)+\sum_k[2JSz-\mu gH+S(K_1+K_2)]a_k^\dagger a_k$$
$$+\sum_k[2JSz+\mu gH+S(K_1+K_2)]b_k^\dagger b_k+\tfrac{1}{2}(K_1-K_2)\sum_k(a_k a_{-k}+a_k^\dagger a_{-k}^\dagger+b_k b_{-k}+b_k^\dagger b_{-k}^\dagger) ,$$

$$\mathcal{H}_2=\Bigg[-\frac{Jz}{2N}\sum_{k_1\cdots k_4}[\gamma_{k_1}a_{k_1}b_{k_2}^\dagger b_{k_3}b_{k_4}\delta_{k_1+k_2,k_3+k_4}+(\gamma_{k_1}b_{k_1}^\dagger a_{k_2}^\dagger a_{k_3}a_{k_4}+2\gamma_{k_1-k_2}a_{k_1}^\dagger a_{k_2}b_{k_3}^\dagger b_{k_4})\delta_{k_1+k_4,k_2+k_3}]$$
$$-\frac{K_1+K_2}{4N}\sum_{k_1\cdots k_4}[(a_{k_1}^\dagger a_{k_2}a_{k_3}^\dagger a_{k_4}+b_{k_1}^\dagger b_{k_2}b_{k_3}^\dagger b_{k_4})\delta_{k_1+k_3,k_2+k_4}]$$
$$-\frac{K_1-K_2}{4N}\sum_{k_1\cdots k_4}(a_{k_1}^\dagger a_{k_2}a_{k_3}a_{k_4}+b_{k_1}^\dagger b_{k_2}b_{k_3}b_{k_4})\delta_{k_1+k_2,k_3+k_4}\Bigg]+\text{Hermitian conjugate} , \tag{A2}$$

where $z$ is once again the number of nearest neighbors, $N$ is the number of spins in each sublattice and $\lambda_k = \sum_{\delta} e^{ik'\delta}/z$. We will first diagonalize the quadratic part of the Hamiltonian $\mathcal{H}_1$. To do this we employ the Bogoliubov transformation

$$\alpha_k = u_1 a_k + u_2 a_{-k}^{\dagger} + u_3 b_k^{\dagger} + u_4 b_{-k} \ . \tag{A3}$$

First, denote

$$A_k = 2JSz\lambda_k \ ,$$
$$B = 2JS_z + S(K_1 + K_2) - \mu gH \ ,$$
$$C = 2JS_z + S(K_1 + K_2) + \mu gH \ ,$$
$$D = S(K_1 - K_2) \ .$$

Solving the secular equation we get the roots

$$\omega_{k,1} = [\tfrac{1}{2}(B^2 + C^2 - 2A_k^2 - 2D^2 + \{(B-C)^2[(B+C)^2 - 4A_k^2] + 16A_k^2 D^2\}^{1/2})]^{1/2} \ ,$$
$$\omega_{k,2} = [\tfrac{1}{2}(B^2 + C^2 - 2A_k^2 - 2D^2 - \{(B-C)^2[(B+C)^2 - 4A_k^2] + 16A_k^2 D^2\}^{1/2})]^{1/2} \ ,$$
$$\omega_{k,3} = \omega_{k,1} \ ,$$
$$\omega_{k,4} = -\omega_{k,2} \ .$$

Solving for the values of $u_1$, $u_2$, $u_3$, and $u_4$ we get

$$u_{1,i} = \frac{A_k D(B + C + 2\omega_{k,i})u_{4,i}}{(\omega_{k,i} + C)(B^2 - \omega_{k,i}^2 - D^2) - A_k^2(\omega_{k,i} + B)} \ ,$$
$$u_{2,i} = \frac{A_k[D^2 - A_k^2 + (B-C)\omega_{k,i} + BC]u_{4,i}}{(\omega_{k,i} + C)(B^2 - \omega_{k,i}^2 - D^2) - A_k^2(\omega_{k,i} + B)} \ , \tag{A4}$$
$$u_{3,i} = \frac{D(B^2 - \omega_{k,i}^2 - D^2 + A_k^2)u_{4,i}}{(\omega_{k,i} + C)(B^2 - \omega_{k,i}^2 - D^2) - A_k^2(\omega_{k,i} + B)} \ ,$$

with $i = 1,2,3,4$. The Bogoliubov transformation is unitary if $[\alpha_k, \alpha_k^{\dagger}] = 1$ or

$$u_{1,i}^2 + u_{4,i}^2 - u_{2,i}^2 - u_{3,i}^2 = 1 \ . \tag{A5}$$

Since we are interested in positive energy solutions only, there are actually only two acceptable energies. It can be readily shown that for values of $S(K_1 - K_2)$ small relative to $2JSz + S(K_1 + K_2)$, which is true for almost all cases, the two positive energies are $\omega_{k,1}$ and $\omega_{k,2}$, which we now denote by $\omega_{k,\pm}$. Then $\mathcal{H}_1$ can be written thus

$$\mathcal{H}_1 = \sum_k (\omega_{k,+}\alpha_k^{\dagger}\alpha_k + \omega_{k,-}\beta_k^{\dagger}\beta_k) \ ,$$

where

$$\alpha_k = u_{1,+}a_k + u_{2,+}a_{-k}^{\dagger} + u_{3,+}b_k^{\dagger} + u_{4,+}b_{-k} \ ,$$
$$\beta_k = u_{1,-}a_k + u_{2,-}a_{-k}^{\dagger} + u_{3,-}b_k^{\dagger} + u_{4,-}b_{-k} \ , \tag{A6}$$

and $u_{i,\pm}$ can be obtained from Eqs. (A4) and (A5). To deal with the pumping term

$$\mathcal{H}_p = \mu gh \cos(\omega_p t)\sum_j S_j^z \ ,$$

which becomes

$$\mathcal{H}_p = \mu gh \cos(\omega_p t)\sum_k (b_k^{\dagger}b_k - a_k^{\dagger}a_k) \tag{A7}$$

and the higher-order terms $\mathcal{H}_2$, we have to invert Eqs. (A6). Once again, we are interested in the long-wavelength limit only so we replace $\lambda_k$ by 1. We get the following:

$$a_k = v_1\alpha_k + v_2\alpha_{-k}^{\dagger} + v_3\beta_k + v_4\beta_{-k}^{\dagger} \ ,$$
$$b_k = w_1\alpha_k^{\dagger} + w_2\alpha_{-k} + w_3\beta_k^{\dagger} + w_4\beta_{-k} \ . \tag{A8}$$

The $v$'s and $w$'s can be obtained in terms of the known $u$'s. All other operators can be obtained from the preceding equations with obvious changes. Then Eq. (A7) produces the pumping terms

$$\mathcal{H}_p = \mu gh\sum_k e^{-i\omega_p t}\{(w_1w_2 - v_1v_2)\alpha_k^{\dagger}\alpha_{-k}^{\dagger} + (w_3w_4 - v_3v_4)\beta_k^{\dagger}\beta_{-k}^{\dagger} + (w_1w_4 + w_2w_3 - v_1v_4 - v_2v_3)\alpha_k^{\dagger}\beta_{-k}^{\dagger}\} + \text{Hermitian conjugate} \ .$$

For typical values of $JSz$, $SK_1$, and $SK_2$, for example, $CuCl_2 \cdot 2H_2O$, we have[23]

$$2JSz = 2150 \times 10^{-18} \text{ ergs} \ ,$$
$$SK_1 = 7.3 \times 10^{-18} \text{ ergs} \ , \tag{A9}$$
$$SK_2 = 2.1 \times 10^{-18} \text{ ergs} \ .$$

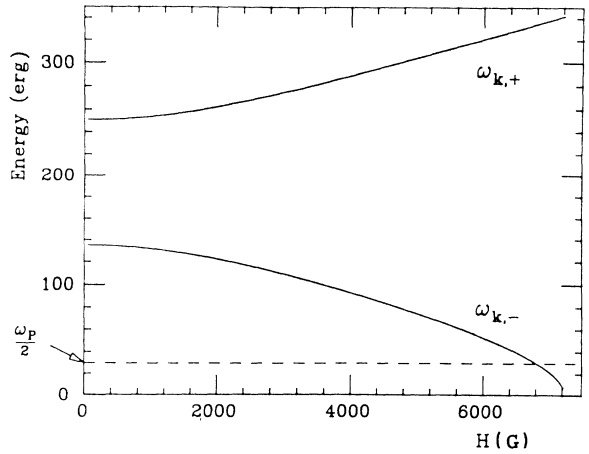


FIG. 10. Plot of $\omega_{k,\pm}$ vs Zeeman field $H$ in the long-wavelength limit. Parameter values appropriate to $CuCl_2 \cdot 2H_2O$.

Using these numbers, we can show how the long-wavelength magnon energies vary with the Zeeman field. Such a variation is shown in Fig. 10 which is a plot of $\omega_{k,\pm}$ versus the Zeeman field $H$ in the long-wavelength limit.

From the typical experimental values of pumping frequencies and applied static fields (see, for example, Ref. 24 for $CuCl_2 \cdot 2H_2O$) we find that only the lower-branch ($k \approx 0$) magnons are excited. So for our analysis, we can neglect the upper branch completely and retain only terms related to the lower branch. Then

$$\mathcal{H}_1+\mathcal{H}_p=\sum_k \omega_{k,-}\alpha_k^\dagger\alpha_k+\mu gh(w_1w_2-v_1v_2)\sum_k (e^{i\omega_p t}\alpha_k^\dagger\alpha_{-k}^\dagger+e^{i\omega_p t}\alpha_k\alpha_{-k}) ,$$

which is already the same as the ferromagnetic case already considered. We now deal with the higher-order terms $\mathcal{H}_2$. From Eqs. (A2) and (A8), after much algebra where only operators involving $\alpha_k^\dagger$ and $\alpha_k$ which are number conserving (scattering terms only) are kept, we finally arrive at the result

$$\mathcal{H}_2=T\sum_{k_1,\ldots,k_4}\alpha_{k_1}^\dagger\alpha_{k_2}^\dagger\alpha_{k_3}\alpha_{k_4}\delta_{k_1+k_2,k_3+k_4}$$

with

$$T=\frac{Jz}{2N}[2(v_1w_1+v_2w_2)(v_1^2+v_2^2+w_1^2+w_2^2)+2v_1w_1(v_2^2+w_2^2)+2v_2w_2(v_1^2+w_1^2)+(v_1^2+v_2^2)(w_1^2+w_2^2)+2v_1v_2w_1w_2]$$
$$-\frac{K_1+K_2}{2N}[v_1^4+v_2^4+w_1^4+w_2^4+4v_1^2v_2^2+4w_1^2w_2^2]-\frac{3(K_1-K_2)}{2N}[v_1v_2(v_1^2+v_2^2)+w_1w_2(w_1^2+w_2^2)] .$$

Once again, we note that in this long-wavelength limit, there is no $k$ dependence to the coefficients. The total Hamiltonian is now

$$\mathcal{H}=\sum_k \omega_{k,-}\alpha_k^\dagger\alpha_k+V\sum_k(e^{-i\omega_p t}\alpha_k^\dagger\alpha_{-k}^\dagger+e^{i\omega_p t}\alpha_k\alpha_{-k})+T\sum_{k_1\cdots k_4}\alpha_{k_1}^+\alpha_{k_2}^+\alpha_{k_3}\alpha_{k_4}\delta_{k_1+k_2,k_3+k_4} ,$$

where $V=\mu gh(w_1w_2-v_1v_2)$ which is a constant. This equation assumes the same form as the easy plane ferromagnet (see Ref. 15) but with different expressions for $\omega_k$, $V$, and $T$. Therefore, provided the conditions are such that only the lower branch of a two-sublattice antiferromagnet is excited, essentially similar behavior should be obtained as in the ferromagnetic case discussed in the main text.

*Current address: Department of Physics, West Virginia University, Morgantown, WV 26506.

[1]R. W. Damon, Rev. Mod. Phys. **25**, 239 (1953).
[2]N. Bloembergen and S. Wang, Phys. Rev. **93**, 72 (1954).
[3]H. Suhl, J. Phys. Chem. Solids **1**, 209 (1957).
[4]V. E. Zakharov, V. S. L'vov, and S. S. Starobinets, Zh. Eksp. Teor. Fiz. **59**, 1200 (1970) [Sov. Phys. JETP **22**, 656 (1971)] See also V. E. Zakharov, V. S. L'vov, and S. L. Musher, Fiz. Tverd. Tela **14**, 832 (1972) [Sov. Phys. Solid State **14**, 710 (1972)]. This reference contains a brief discussion of mode limitation from a different point of view.
[5]K. Nakamura, S. Ohta, and K. Kawasaki, J. Phys. C **15**, L143 (1982). See also S. Ohta and K. Nakamura, *ibid.* **16**, L605 (1983).
[6]G. Gibson and C. Jeffries, Phys. Rev. A **29**, 811 (1984).
[7]S. M. Rezende, F. M. de Aquiar, and D. F. de Alcantara Bomfim, J. Magn. Magn. Mater. **54-57**, 1127 (1986).
[8]F. M. de Aquiar and S. M. Rezende, Phys. Rev. Lett. **56**, 1070 (1986).
[9]M. Mino and H. Yamazaki, J. Phys. Soc. Jpn. **55**, 4168 (1986).
[10]P. Bryant, C. Jeffries, and K. Nakamura, Phys. Rev. Lett. **60**, 1185 (1988).
[11]X. Y. Zhang and H. Suhl, Phys. Rev. A **32**, 2530 (1985).
[12]S. M. Rezende, O. F. de Alcantara Bonfim, and F. M. de Aquiar, Phys. Rev. B **33**, 5153 (1986).
[13]H. Suhl and C. Y. Zhang, Phys. Rev. Lett. **57**, 1480 (1986).
[14]T. L. Gill and W. W. Zachary, J. Appl. Phys. **61**, 4130 (1987).
[15]S. P. Lim and D. L. Huber, Phys. Rev. B **37**, 5426 (1988).
[16]S. P. Lim and D. L. Huber, J. Appl. Phys. **63**, 4151 (1988).
[17]V. E. Zakharov, V. S. L'vov, and S. S. Starobinets, Usp. Fiz. Nawk. **114**, 609 (1974) [Sov. Phys. Usp.—**17**, 896 (1975)].
[18]I. S. Gradshteyn and I. M. Ryzhik, *Tables of Integrals, Series and Products* (Academic, Orlando, 1980), p. 148.
[19]The dependence of the occupation numbers of the individual modes on the initial conditions is to be expected in the absence of "noise terms" in the equations of motion.
[20]H. Suhl and X. Y. Zhang, J. Appl. Phys. **63**, 4147 (1988).
[21]X. Y. Zhang and H. Suhl, Phys. Rev. B **38**, 4893 (1988).
[22]J. Carr, *Applications of Center Manifold Theory* (Springer-Verlag, New York, 1984), Vol. 28.
[23]R. J. Joenk, Phys. Rev. **126**, 565 (1962); *ibid.* **127**, 2287 (1963).
[24]H. Yamazaki, J. Phys. Soc. Jpn. **53**, 1155 (1984).